Chapter 8
Rational Bézier Formulas with Quaternion and Clifford Algebra Weights

Rimvydas Krasauskas and Severinas Zubė

8.1 Introduction

Bézier curves and surfaces are widely used in computer graphics and computer-aided design. Their formulas are affine invariant and depend on control points that are visually intuitive and convenient for many applications. On the other hand, there is an important class of primitive surfaces (spheres, rotational cylinders, rotational cones, and tori) with specific properties that are not intrinsic to their classical Bézier representation. For example, one simple reason is the lack of affine invariance.

An alternative theory for curves on a plane was introduced by Sanchez-Reyes in [20]: complex rational Bézier curves were defined using complex numbers for control points and weights. This complex Bézier approach has two main advantages:

- More compact representation: the degree is halved (e.g. circles have linear form);
- Invariance with respect to Möbius transformations.

In order to extend this theory of complex planar curves to surfaces in space we use quaternions and follow the quaternion representation of circles in space [21]. Here one can hardly expect a theory as complete as in the planar case. Indeed, as the quaternion algebra $\mathbb{H}$ is 4-dimensional, one needs to take extra care to ensure that resulting surfaces are contained in the 3-dimensional subspace in $\mathbb{H}$ which is identified with $\mathbb{R}^3$. Also tools for intuitive shape manipulation are still under development.

Of course, there is one notable exception: the case of spherical quaternion curves and surface patches can be reduced to the complex planar case (because a sphere is

R. Krasauskas (✉) • S. Zubė
Vilnius University, Vilnius, Lithuania
e-mail: rimvydas.krasauskas@mif.vu.lt; severinas.zube@mif.vu.lt

T. Dokken, G. Muntingh (eds.), *SAGA – Advances in ShApes, Geometry, and Algebra*, Geometry and Computing 10, DOI 10.1007/978-3-319-08635-4_8

Möbius equivalent to a plane). We only sketch the spherical case in Sect. 8.2.5. and postpone the details to a separate publication.

The first part of the current chapter (Sects. 8.2–8.3) is devoted to the simplest non-trivial case of a quaternion surface, namely a bilinear Quaternion–Bézier (QB) patch. Arbitrary bilinear QB surface patches are characterized as special Darboux cyclide patches using a recent exposition of the classical theory of Darboux cyclides in [19]. Actually, the results of the unpublished manuscript [13] are presented here with extended proofs and more details about Möbius transformations. Note that these new formulas not only reproduce earlier known biquadratic parametrizations of principal patches of Dupin cyclides (considered, e.g. in [2, 11]), but also define totally unknown patches on general Darboux cyclides, which can hardly be generated using the customary Bézier approach.

The second part of the chapter is targeted to a reader who has certain acquaintance with geometric (Clifford) algebras and the isotropic model of Laguerre geometry. Similar Bézier-like formulas make sense in higher dimensional pseudo-Euclidean spaces if quaternions are replaced with elements of the corresponding geometric algebra. Section 8.4 is devoted to general Clifford–Bézier formulas and recent research: the conformal model of Euclidean space, isotropic geometry and isotropic cyclides, and applications to PN-surface modeling.

8.2 Quaternionic Bézier Formulas

8.2.1 Quaternions

We will use the algebra of quaternions $\mathbb{H}$ with the standard basis $\mathbf{1}$, i, j, k:

$$\mathrm{i}^2 = \mathrm{j}^2 = \mathrm{k}^2 = -\mathbf{1}, \quad \mathrm{ij} = \mathrm{k}, \quad \mathrm{jk} = \mathrm{i}, \quad \mathrm{ki} = \mathrm{j}.$$

Reals $\mathbb{R}$ and the 3-dimensional space $\mathbb{R}^3$ will be identified with the *real* and the *imaginary* vector subspaces of $\mathbb{H}$:

$$\mathbb{R} = \mathrm{Re}\,\mathbb{H}, \quad r \mapsto r\mathbf{1}, \qquad \mathbb{R}^3 = \mathrm{Im}\,\mathbb{H}, \quad v \mapsto v_1\mathrm{i} + v_2\mathrm{j} + v_3\mathrm{k}.$$

It will be convenient to decompose a quaternion $q \in \mathbb{H}$ into its scalar (real) part and its vector (imaginary) part:

$$q = r + v = r\mathbf{1} + v_1\mathrm{i} + v_2\mathrm{j} + v_3\mathrm{k}, \quad r = \mathrm{Re}(q), \quad v = \mathrm{Im}\,(q).$$

The quaternionic product in this notation has the following compact formula:

$$qq' = (r + v)(r' + v') = (rr' - v \cdot v') + (rv' + r'v + v \times v'),$$

where $v \cdot v'$ and $v \times v'$ are dot and vector products in $\mathbb{R}^3$.

If $q = r + v$ then $\bar{q} = r - v$ is a conjugate quaternion, $|q| = \sqrt{q\bar{q}}$ is its length, and $q^{-1} = \bar{q}/|q|^2$ is the inverse of q. In particular, if $v \in \operatorname{Im} H$ then $\bar{v} = -v$ and $v^{-1} = -v/|v|^2$.

8.2.2 *Möbius Transformations in* $\mathbb{R}^3$

Möbius (M) transformations in space are generated by inversions in $\mathbb{R}^3$ with respect to spheres. Alternatively, after identifying R^3 with the subset $\operatorname{Im}\mathbb{H}$ of imaginary quaternions, M-transformations can be generated by four kinds of elementary transformations: reflections, translations, dilatations, and special inversions (with unit radius and center in the origin)

$$R_v(x) = -vxv, \quad T_a(x) = x + a, \quad S_r(x) = rx, \quad \operatorname{inv}(x) = -x^{-1}, \tag{8.1}$$

where $v, a \in \operatorname{Im}\mathbb{H}$, $|v| = 1$, $r \in \mathbb{R}_+$. The composition of an even number of reflections is a rotation.

M-transformations can be represented as fractional-linear functions Φ_A associated with a 2×2 matrix A with quaternion entries:

$$\Phi_A(x) = (ax + b)(cx + d)^{-1}, \quad A = \begin{pmatrix} a & b \\ c & d \end{pmatrix}. \tag{8.2}$$

Usual multiplication of matrices (multiplication of their elements should be in natural order!) corresponds to composition of fractional-linear functions. For example, elementary transformations Eq. (8.1) correspond to the following matrices

$$\begin{pmatrix} v & 0 \\ 0 & v \end{pmatrix}, \quad \begin{pmatrix} 1 & a \\ 0 & 1 \end{pmatrix}, \quad \begin{pmatrix} r & 0 \\ 0 & 1 \end{pmatrix}, \quad \begin{pmatrix} 0 & -1 \\ 1 & 0 \end{pmatrix}. \tag{8.3}$$

From [3, Theorem 11.1] it follows that the map $A \mapsto \Phi_A$ defines a surjective homomorphism of the matrix group

$$\mathrm{GL}(\operatorname{Im}\mathbb{H}) = \left\{ \begin{pmatrix} a & b \\ c & d \end{pmatrix} \mid \operatorname{Re}(a\bar{c}) = \operatorname{Re}(b\bar{d}) = 0,\ \bar{b}c + \bar{d}a \in \mathbb{R}^* \right\}, \quad \mathbb{R}^* = \mathbb{R} \setminus \{0\},$$

to the group of M-transformations of $\operatorname{Im}\mathbb{H}$.

For any for points $p_0, \ldots, p_3 \in \operatorname{Im}\mathbb{H}$ we define a *cross-ratio*

$$\operatorname{cr}(p_0, p_1, p_2, p_3) = (p_0 - p_1)(p_1 - p_2)^{-1}(p_2 - p_3)(p_3 - p_0)^{-1}. \tag{8.4}$$

There is a full analog of the well-known fact that four complex points lie on a circle only if their cross-ratio is real.

Proposition 8.1 ([4]) *A cross-ratio* $\mathrm{cr}(p_0, p_1, p_2, p_3)$ *is real if and only if these four points are on a circle. A real cross-ratio is Möbius invariant.*

8.2.3 Properties of Quaternionic Bézier Formulas

A *quaternionic Bézier (QB) formula* is a fraction of two linear combinations of control points and weights $p_i, w_i \in \mathbb{H}$ with coefficients B_i

$$F = \left(\sum_i p_i w_i B_i\right)\left(\sum_i w_i B_i\right)^{-1}.$$

The coefficients B_i can be the following Bernstein polynomials:

- $B_i^d(t) = \binom{d}{i}(1-t)^{d-i}t^i$, $i = 0, \ldots, d$ define *QB curves* of degree d;
- $B_i^{d_1}(s)B_j^{d_2}(t)$, $i = 0, \ldots, d_1$, $j = 0, \ldots, d_2$, define *QB tensor product surfaces* of bidegree (d_1, d_2);
- $B_{ij}^d = \frac{d!}{(d-i-j)!i!j!}(1-s-t)^{d-i-j}s^i t^j$, with integers $i \geq 0$, $j \geq 0$, $i + j \leq d$, define *QB triangular surfaces* of degree d.

General QB formulas take values in the 4-dimensional space of quaternions $\mathbb{H}$. The most interesting space for us will be $\mathbb{R}^3$, which is identified with $\mathrm{Im}\,\mathbb{H}$. Therefore, we always need to ensure that the QB curves and surfaces under consideration are contained in $\mathrm{Im}\,\mathbb{H}$.

Proposition 8.2 *A QB formula* $F = (\sum_i p_i w_i B_i)(\sum_i w_i B_i)^{-1}$ *is invariant with respect to Möbius transformations: if* $\Phi = \Phi_A$ *defined by* (8.2) *then*

$$\Phi(F) = (\textstyle\sum_i p_i' w_i' B_i)(\sum_i w_i' B_i)^{-1}, \quad p_i' = \Phi(p_i),\ w_i' = \hat{\Phi}(p_i, w_i) = (cp_i + d)w_i.$$

If $F \in \mathrm{Im}\,\mathbb{H}$ *then* $\Phi(F) \in \mathrm{Im}\,\mathbb{H}$.

Proof It is easy to check this directly using the identities

$$\Phi(xy^{-1}) = (ax + by)(cx + dy)^{-1}, \quad p_i' w_i' = \Phi(p_i)\Phi(p_i, w_i) = (ap_i + b)w_i.$$

□

This proposition allows us to calculate Möbius transformations of any rational Bézier curves and surfaces (with real weights) and get a lot of new non-trivial examples of QB curves and surfaces in $\mathrm{Im}\,\mathbb{H}$.

Remark 8.1 Möbius deformations of 3D models were realized on GPU using real time evaluations of quaternion formulas in [9] (see Fig. 8.1). Since such transformations are conformal, they may be convenient for deforming organic shapes including textures.

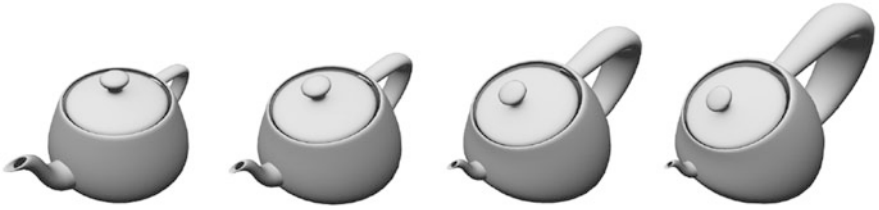

Fig. 8.1 Möbius transformation of the Utah Teapot [9]

In general the quaternion representation has half the degree of the customary rational Bézier case with real weights.

Proposition 8.3 *A QB formula* $F = (\sum_i p_i w_i B_i)(\sum_i w_i B_i)^{-1}$ *of degree* d *(resp. bidegree* (d_1, d_2)*) defines the same parametrization as the following Bézier formula of degree* $2d$ *(resp. bidegree* $(2d_1, 2d_2)$*)*

$$\tilde{F} = (N\bar{D})(D\bar{D})^{-1}, \quad N = \sum_i p_i w_i B_i, \quad D = \sum_i p_i w_i B_i.$$

Proof Note that the new numerator $N\bar{D}$ and denominator $D\bar{D}$ can both be expanded in the new basis $\{B_i B_j\}$ and $D\bar{D}$ is real. □

8.2.4 Circular Arcs

Here we reformulate some results of [21] about the quaternionic representation of a circle and give proofs based on Propositions 8.2 and 8.3.

Let p_0 and p_1 be the two endpoints of a circular arc C in $\mathbb{R}^3 = \operatorname{Im}\mathbb{H}$, and let p_∞ be some point on the complementary arc of C. We are going to parametrize this arc rationally in three steps:

- Apply the inversion $I : x \mapsto p_\infty - (x - p_\infty)^{-1}$ with the center in p_∞ to the circle C;
- Parametrize the resulting line segment $L(t) = I(p_0)(1-t) + I(p_1)t$;
- Apply the same inversion once more $C(t) = I(L(t))$.

The inversion I is a composition $T_{p_\infty} \circ \mathrm{inv} \circ T_{-p_\infty}$ of elementary transformations (8.1) and has the following matrix representation (see (8.3))

$$\begin{pmatrix} 1 & p_\infty \\ 0 & 1 \end{pmatrix} \begin{pmatrix} 0 & -1 \\ 1 & 0 \end{pmatrix} \begin{pmatrix} 1 & -p_\infty \\ 0 & 1 \end{pmatrix} = \begin{pmatrix} p_\infty & -1 - p_\infty^2 \\ 1 & -p_\infty \end{pmatrix}.$$

According to Proposition 8.2, a linear Bézier curve $L(t)$ with control points $I(p_0)$, $I(p_1)$ and unit weights is transformed to a linear QB curve with control points

$I(I(p_i)) = p_i$, and weights $w_i = I(p_i) - p_\infty = -(p_i - p_\infty)^{-1}$, $i = 0, 1$. So we finally get the parametrization of the circular arc

$$C(t) = (p_0 w_0(1-t) + p_1 w_1 t)(w_0(1-t) + w_1 t)^{-1}, \tag{8.5}$$

that is contained in Im $\mathbb{H}$ by construction.

Remark 8.2 One can divide both weights in (8.5) by w_0 and get the equivalent pair of weights $w_0' = 1$ and $w_1' = w_1 w_0^{-1}$. If just one weight is multiplied by a real number $\lambda > 0$ then the arc is reparametrized.

Remark 8.3 The parameter t in $C(t)$ has a simple interpretation as a cross-ratio

$$t = \mathrm{cr}(p_\infty, p_1, p_0, C(t)). \tag{8.6}$$

Indeed, according to Proposition 8.1 it is enough to check the following much simpler identity $\mathrm{cr}(\infty, I(p_1), I(p_0), L(t)) = t$, where $\infty = I(p_\infty)$ is the infinite point of Im $\mathbb{H}$.

The customary Bézier representation of $C(t)$ can be derived using Proposition 8.3: denote the numerator of the fraction (8.5) by N and the denominator by D, then rewrite this fraction as $C(t) = ND^{-1} = N\bar{D}(D\bar{D})^{-1}$ with a real denominator, and expand both $N\bar{D}$ and $D\bar{D}$ in the quadratic Bernstein basis B_i^2, $i = 0, 1, 2$:

$$N\bar{D} = p_0 w_0 \bar{w}_0 B_0^2 + \frac{1}{2}(p_0 w_0 \bar{w}_1 + p_1 w_1 \bar{w}_0) B_1^2 + p_2 w_2 \bar{w}_2 B_2^2,$$

$$D\bar{D} = w_0 \bar{w}_0 B_0^2 + \frac{1}{2}(w_0 \bar{w}_1 + w_1 \bar{w}_0) B_1^2 + w_2 \bar{w}_2 B_2^2.$$

Hence $C(t)$, as a quadratic rational Bézier curve, has real weights

$$W_0 = w_0 \bar{w}_0, \quad W_1 = \frac{1}{2}(w_0 \bar{w}_1 + w_1 \bar{w}_0) = \mathrm{Re}(w_0 \bar{w}_1), \quad W_2 = w_1 \bar{w}_1, \tag{8.7}$$

and control points

$$P_0 = p_0, \quad P_1 = \frac{p_0 w_0 \bar{w}_1 + p_1 w_1 \bar{w}_0}{w_0 \bar{w}_1 + w_1 \bar{w}_0}, \quad P_2 = p_1. \tag{8.8}$$

We can also calculate a tangent vector v_0 to $C(t)$ at p_0 as a derivative $C'(0)$ at $t = 0$. First we differentiate the identity $N = CD$ and get $N' = C'D + CD'$. Then $C'(0) = (N'(0) - C(0)D'(0))D(0)^{-1} = (p_1 w_1 - p_0 w_0 - p_0(w_1 - w_0))w_0^{-1}$ and

$$v_0 = C'(0) = (p_1 - p_0) w_1 w_0^{-1}. \tag{8.9}$$

Therefore, the weights cannot be arbitrary. The following relations between weights and control points will be useful later.

Proposition 8.4 *If C is a QB curve (8.5) with $p_0, p_1 \in \mathrm{Im}\,\mathbb{H}$ then:*

$$C \subset \mathrm{Im}\,\mathbb{H} \Leftrightarrow \mathrm{Re}(p_0 w_0 \bar{w}_1 + p_1 w_1 \bar{w}_0) = 0 \tag{8.10}$$

$$C \subset \mathrm{Im}\,\mathbb{H} \Leftrightarrow \mathrm{Im}\,(w_1 w_0^{-1}) \perp (p_1 - p_0) \tag{8.11}$$

$$C \text{ is a line} \Leftrightarrow w_1 w_0^{-1} \in \mathbb{R} \tag{8.12}$$

If $C \subset \mathrm{Im}\,\mathbb{H}$ and $u = \mathrm{Im}\,(w_1 w_0^{-1}) \neq 0$ then C is a circle in a plane orthogonal to u.

Proof The circle C is contained in $\mathrm{Im}\,\mathbb{H}$ if and only if its middle control point P_1 is there, i.e. $\mathrm{Re}\,P_1 = 0$. From its expression in (8.8) condition (8.10) follows. This is also equivalent to $v_0 \in \mathrm{Im}\,\mathbb{H}$, so $(p_1 - p_0) w_1 w_0^{-1} \in \mathrm{Im}\,\mathbb{H}$ (see (8.9)) and (8.11) follows. Similarly (8.12) and the last statement can be derived from (8.9). □

8.2.5 *Spherical Quaternionic Bézier Curves and Surface Patches*

In this section we sketch the theory of QB curves and surfaces on a sphere (or plane), by reducing quaternionic-Bézier formulas to complex-Bézier formulas.

Let us start with the simplest surface example. A spherical triangle with corner points p_0, p_1, p_2 bounded by three circular arcs (such that these three circles intersect in a point p_∞) has the parametrization formula with weights: $w_i = -(p_i - p_\infty)^{-1}$, $i = 0, 1, 2$, (see Fig. 8.2, left)

$$T(s,t) = (p_0 w_0 (1-s-t) + p_1 w_1 s + p_2 w_2 t)(w_0(1-s-t) + w_1 s + w_2 t)^{-1}. \tag{8.13}$$

Indeed this is the Möbius image of a planar linear Bézier triangle (cf. Sect. 8.2.4).

In order to generalize this example we introduce two different inclusions of $\mathbb{C}$ into $\mathbb{H}$ (which are compatible with geometric algebra formulas in Sect. 8.4.3)

$$\mathrm{in}_1 : \mathbb{C} \to \mathbb{H},\ x + y\mathrm{i} \mapsto x - y\mathrm{k}, \quad \mathrm{in}_2 : \mathbb{C} \to \mathrm{Im}\,\mathbb{H},\ x + y\mathrm{i} \mapsto x\mathrm{i} + y\mathrm{j}. \tag{8.14}$$

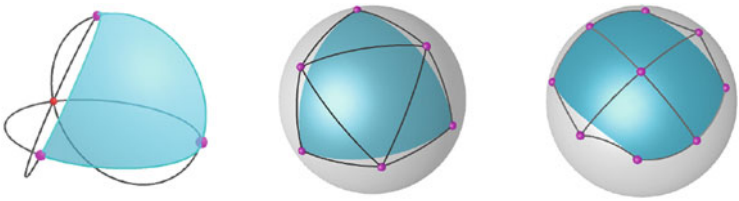

Fig. 8.2 Spherical QB-patches: linear and quadratic triangle, biquadratic quad patch

Then any complex-Bézier formula $(\sum_i p_i w_i B_i)(\sum_i w_i B_i)^{-1}$, $p_i, w_i \in \mathbb{C}$, can be transformed to a QB formula $(\sum_i p'_i w'_i B_i)(\sum_i w'_i B_i)^{-1}$, $w'_i = \mathrm{in}_1(w_i)$, $p'_i = \mathrm{in}_2(p_i)$, on the plane $z = 0$ or on any sphere in $\mathrm{Im}\,\mathbb{H}$ by Möbius invariance according to Proposition 8.2. Hence the whole theory of complex Bézier curves on a plane developed in [20] can be translated into QB form and then extended to any sphere.

Even more, it appears that all rational Bézier curves and surface patches on a sphere can be represented in QB form of halved degree. The following theorem can be proved using generalized stereographic projection [6] and its interpretation in terms of complex projective line [10].

Theorem 8.1 *Any rational Bézier curve or triangular (resp. rectangular) surface patch of degree $2d$ (resp. of bidegree $(2d_1, 2d_2)$) on a sphere $S^2 \subset \mathrm{Im}\,\mathbb{H}$ can be represented in a quaternionic Bézier form of degree d (resp. of bidegree (d_1, d_2)) with the control net composed of circular arcs lying on S^2.*

Figure 8.2 (middle and right) illustrates a QB-triangle of degree 2 (which is a spherical octant) and a biquadratic QB-rectangle.

The quaternionic approach allows us to deal with all spheres in $\mathbb{R}^3$ in the unique framework. In a certain sense every sphere carries its own complex structure that is encoded in global quaternionic structure.

8.3 Bilinear Quaternionic Bézier Patches

We do not know much about general QB curves and surfaces, so we are going to study important particular cases.

Remark 8.4 Non-spherical QB-curves of degree 2 in $\mathrm{Im}\,\mathbb{H}$ are characterized in [22] as the diagonals $P(t,t)$ of bilinear QB-surfaces defined by (8.15). Note that the middle control point of such curves is not contained in $\mathrm{Im}\,\mathbb{H}$.

The simplest cases of QB surfaces are linear triangles and bilinear quadrangles. The first case will turn out to be spherical, hence we will focus on the latter.

Proposition 8.5 *Any linear QB triangle in $\mathrm{Im}\,\mathbb{H}$ is spherical.*

Proof Consider the formula of a QB triangular patch (8.13), and apply inversion with center on the boundary circle going through p_0 and p_1 that transforms this circle into a line. Using the same notation for control points and weights, one can assume $w_0 = w_1 = 1$ (see Remark 8.2 and (8.12)). Then it follows from Proposition 8.4 that $\mathrm{Im}\,(w_2)$ is orthogonal to a family of circles with control points $q(s) = p_0(1-s) + p_1 s$, p_2 and weights 1, w_2, that cover the patch. Hence, this inversion of the initial triangular patch is planar. □

8.3.1 Properties of Bilinear QB-Patches

Let us define a bilinear QB-quadrangular patch (call it just a bilinear QB-patch) with slightly different indexing (the fraction is used in the sense $\frac{a}{b} = ab^{-1}$):

$$P(s,t) = \frac{p_0 w_0 (1-s)(1-t) + p_1 w_1 s(1-t) + p_2 w_2 (1-s)t + p_3 w_3 st}{w_0(1-s)(1-t) + w_1 s(1-t) + w_2(1-s)t + w_3 st}, \tag{8.15}$$

We consider only the case when the image is contained in $\operatorname{Im} \mathbb{H} = \mathbb{R}^3$.

Lemma 8.1 *If two adjacent boundary circles of a bilinear QB-patch P defined by (8.15) are cospherical then the patch is either spherical or a patch of a double ruled quadrics (including its Möbius transformations).*

Proof Denote by C_{ij}, $ij = 01, 02, 13, 23$, the boundary circles connecting adjacent points p_i and p_j. If circles C_{01} and C_{02} are cospherical then there are two cases: (a) they intersect in two points p_0 and $q \neq p_0$; (b) they are tangent in p_0 (a double point).

In case (a) we apply inversion with a center q and use the same notation for the transformed patch. Now C_{01} and C_{02} are line segments, and one can assume (after a reparametrization) $w_0 = w_1 = w_2 = 1$ (see (8.12)). If $w_3 \in \mathbb{R}$ then the patch P is on a bilinear quadric (or plane). Otherwise $\operatorname{Im}(w_3) \neq 0$, and according to Proposition 8.4 $\operatorname{Im}(w_3) \perp (p_3 - p_1)$ and $\operatorname{Im}(w_3) \perp (p_3 - p_2)$. Hence the two boundary circles C_{13} and C_{23} lie on the same plane Π going through three points p_1, p_2, p_3. All the weights along these circles have the same direction, since they are linear averages between w_3 and 1. Similarly it follows that all other circles on P are on the same plane Π, and P is planar, i.e. spherical. Case (b) can be treated similarly: apply an inversion with center p_0 and notice that despite the blown-up corner p_0 the same arguments are valid. □

Lemma 8.2 *Let four circles C_{ij}, $ij = 01, 02, 13, 23$, in $\operatorname{Im} \mathbb{H}$ be defined by pairs of control points and weights $\{(p_i, w_i), (p_j, w_j)\}$, and suppose that any two adjacent circles are not cospherical. Then there is a unique non-zero number*

$$\lambda = -\operatorname{Re}(p_1 w_1 \bar{w}_2 + p_2 w_2 \bar{w}_1)\big(\operatorname{Re}(p_0 w_0 \bar{w}_3 + p_3 w_3 \bar{w}_0)\big)^{-1} \in \mathbb{R}, \tag{8.16}$$

such that the same control points with weights w_0, w_1, w_2, λw_3 define a bilinear QB-patch in $\operatorname{Im} \mathbb{H} = \mathbb{R}^3$.

Proof Denoting numerator and denominator in formula (8.15) with control points $p_i, i = 0, \ldots, 3$, and weights $w_0, w_1, w_2, \lambda w_3$ by N and D, we can modify it to the form with a real denominator $P = ND^{-1} = N\overline{D}(D\overline{D})^{-1}$. Then we expand $N\overline{D}$ in a biquadratic Bernstein basis and get control points (multiplied by their weights) of the corresponding rational biquadratic Bézier surface. Boundary control points are

obviously in $\mathrm{Im}\,\mathbb{H}$, since they represent circular arcs in $\mathrm{Im}\,\mathbb{H}$. The middle control point multiplied by its weight has the following form:

$$q_{11} = (p_1 w_1 \bar{w}_2 + p_2 w_2 \bar{w}_1) + \lambda(p_0 w_0 \bar{w}_3 + p_3 w_3 \bar{w}_0),$$

where both expressions in brackets have non-zero real parts (otherwise, adjacent boundary circles will be cospherical, cf. the proof of Proposition 8.5 and formula (8.10)). Solving the equation $\mathrm{Re}(q_{11}) = 0$ for λ we get exactly (8.16). □

Lemma 8.3 *Let C_{02}, C_{01}, C_{13} be circles in $\mathbb{R}^3$, and suppose that $p_0 = C_{02} \cap C_{01}$ and $p_1 = C_{01} \cap C_{13}$ are unique points of their transversal intersection. Then for any other point $p_2 \in C_{02}$, $p_2 \neq p_0$, there exists a unique bilinear QB-patch (up to trivial reparametrization) with control points p_i, $i = 0, 1, 2$, and $p_3 \in C_{13}$ with three boundary arcs lying on the given three circles.*

Proof Our goal is to construct a closed contour of circular quaternionic arcs and then fill the contour using Lemma 8.2.

We choose any point $q \in C_{13}$, $q \neq p_1$, and apply inversion with center q. Using the same notation, we see that C_{13} is a line, and we can find unique (up to real multiplier) weights $w_1 = 1$, w_0 and w_2, that allows us to parametrize the circles C_{01}, C_{02}. The point p_2 and weight w_2 determine a plane Π where a circle C_{23} should be (see Proposition 8.4). So we can find a point p_3 as an intersection $\Pi \cap C_{13}$ with a weight $w_3 = 1$. An exceptional case when Π is parallel to the line C_{13} can happen only when the initial point q (before inversion) can be chosen as p_3. □

8.3.2 Implicitization

We are going to find the implicit equation of the patch (8.15) as an algebraic surface in $\mathbb{R}^3$.

Let us consider a formal equation with a quaternion $X = u + x\mathrm{i} + y\mathrm{j} + z\mathrm{k}$ on the left side and with a bilinear quaternionic patch on the right side:

$$X = N(s,t)D(s,t)^{-1}, \tag{8.17}$$

where $N(s,t)$ and $D(s,t)$ are the numerator and the denominator of the fraction in (8.15). Let us multiply both sides of (8.17) by $D(s,t)$ and move all terms to the left side

$$XD(s,t) - N(s,t) = 0.$$

We treat this quaternionic equation as a system of 4 real linear equations with 4 unknowns

$$(1-s)(1-t), \quad s(1-t), \quad (1-s)t, \quad st.$$

The 4×4 matrix M of this system has 4 columns filled with components of quaternions $(X - p_i)w_i$, $i = 0, \ldots, 3$. Hence the entries of the matrix M are linear forms in u, x, y, z, and the polynomial

$$F(u, x, y, z) = \det\left[(X - p_0)w_0, (X - p_1)w_1, (X - p_2)w_2, (X - p_3)w_3\right] \tag{8.18}$$

must vanish on every point X of the patch $P(s, t)$. Therefore, $F(u, x, y, z) = 0$ defines at most a quartic equation in the variables u, x, y, z.

Theorem 8.2 *Let $P(s, t)$ be the bilinear parametrization of the patch 8.15 in* $\mathrm{Im}\,\mathbb{H} = \mathbb{R}^3$. *Then an implicit equation of the corresponding parameterized surface is a factor of the polynomial $F(0, x, y, z)$ defined by (8.18) and has at most degree* 4.

Example 8.1 A bilinear QB-patch $P(s, t)$ with the following points $[p_0, \ldots, p_3] = [-\mathrm{i}, \mathrm{i}, -\mathrm{i}+\mathrm{j}, \mathrm{i}+\mathrm{j}]$ and weights $[w_0, \ldots, w_3] = [1, \mathrm{j}, 1, \mathrm{j}]$ generates the equation of the cylinder $x^2 + z^2 - 1 = 0$. The same points as above with the weights $(w_0, \ldots, w_3) = (1, \mathrm{j}, \mathrm{k}, \mathrm{i})$ generate the equation of the torus

$$\left(x^2 + \left(y - \frac{1}{2}\right)^2 + z^2 + \frac{3}{4}\right)^2 - 4\,(x^2 + z^2) = 0.$$

All these examples can be classified as Darboux cyclide patches. *Darboux cyclides* are quartic surfaces with a double conic $x^2 + y^2 + z^2 = 0$ at infinity and their Möbius transformations: non-spherical quadrics and cubics with the same double conic. We consider only irreducible cases: for example, a union of two spheres is excluded.

Corollary 8.1 *Any non-spherical bilinear QB-patch is a Darboux cyclide patch.*

Proof According to Theorem 8.2 a bilinear QB-patch has at most degree 4. Since it is Möbius invariant, its arbitrary inversion is also a bilinear QB-patch. These are sufficient conditions for the patch to be on a Darboux cyclide (see details in [15]). □

8.3.3 Bilinear Quaternionic Bézier Patches on Darboux Cyclides

It is known from the theory of Darboux cyclides (see the exposition in [19]) that they can contain at most 6 real families of circles, that are grouped in pairs. Two circles from distinct families intersect in a unique point if these families are from different pairs, otherwise the circles are cospherical [19, Propositions 4, 5]. Any bilinear QB-patch defines a Darboux cyclide by Corollary 8.1 and generates two families of isoparametric circles on it.

Theorem 8.3 *Any two families of circles from different pairs on a given Darboux cyclide are generated by a bilinear QB-patch. Two families of circles from the same*

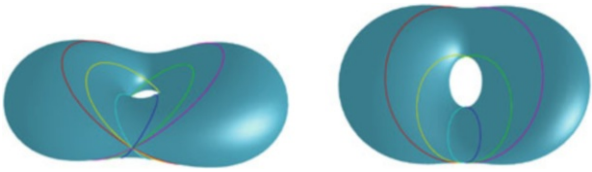

Fig. 8.3 A Darboux cyclide with six circles representing six distinct families

pair can be generated only by a QB-patch defined by rulings of a double ruled quadric (or its Möbius equivalent).

Proof Take two circles C_{02}, C_{13} from one family and one C_{01} from another family that is not in the same pair. Then pairs of circles C_{02}, C_{01} and C_{01}, C_{13} intersect in the unique points p_0 and p_1. Hence we are in the situation of Lemma 8.3 that allows us to construct a bilinear QB-patch bounded by these three circles. So it is enough to prove the uniqueness of a Darboux cyclide going through these circles. Here we can follow [19] and employ the conformal model by lifting the whole construction to a 3-sphere S^3 in the space $\mathbb{R}^4$. Now the circles C_{02}, C_{13} are contained in two 2-planes which intersect in the apex of the quadratic 3-dimensional cone, which cuts our Darboux cyclide in S^3. Let us cut the cone by any hyperplane Π (not containing the apex) and project all circles from the apex to Π. Their images will be two skew lines L_{02}, L_{13} and a conic C'_{01} intersecting them. Therefore the uniqueness problem is reduced to the following simple one: prove the uniqueness of a quadric surface in $\mathbb{R}^3$ going through a given pair of skew lines and one conic. The second part of the theorem follows from Lemma 8.1, since circles from the paired families are cospherical. □

In Fig. 8.3 below we can see an example of a symmetric Darboux cyclide with six paired families of circles (i.e. there are three pairs).

Corollary 8.2 *There are exactly 12 different bilinear QB-patches on a Darboux cyclide with 6 real families of circles.*

Proof Apply Theorem 8.3 and count cases: three choices of two pairs of circle families times four choices of two families from these two distinct pairs. □

8.3.4 Principal Dupin Cyclide Patches

For a definition of a Dupin cyclide see e.g. [5] and references therein. This is a particular case of a Darboux cyclide containing two self-paired families of circles (i.e. both families in a pair coincide, see previous Sect. 8.3.3). A *principle Dupin cyclide patch* is a quadrangular patch bounded by circles from these families (see Fig.8.3), which can be characterized by the following properties:

- All angles are right angles and corner points $p_0, \ldots, p_3$ are on a circle;

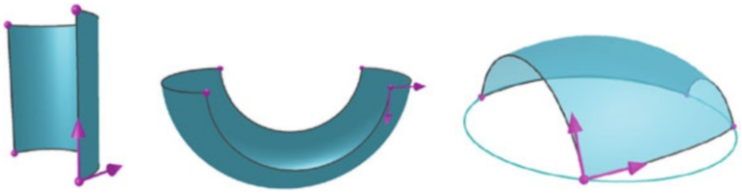

Fig. 8.4 Principal patches on: cilinder, torus, general Dupin cyclide

- Tangent vectors at the end points of the opposite boundary arcs in the adjacent corners are symmetric with respect to a vector joining these points; e.g. let v_{ij} be a tangent vector at p_i pointing to p_j then $v_{23} = -(p_2 - p_0)v_{01}(p_2 - p_0)^{-1}$.

Theorem 8.4 *A principal Dupin cyclide patch with corners in four points $p_0, \ldots, p_3$ on a circle and two orthogonal tangent vectors v_{01} and v_{02} at p_0 can be parametrized by a bilinear QB-patch with these control points and the following weights (where $q_{ij} = (p_i - p_j)/|p_i - p_j|$):*

$$w_0 = 1, \quad w_1 = q_{01}v_{01}, \quad w_2 = q_{02}v_{02}, \quad w_3 = |p_2 - p_1||p_3 - p_0|^{-1}q_{13}w_1q_{20}w_2.$$

The proof of this theorem and other important quaternionic formulas related to principal Dupin cyclide patches can be found in [14] (Fig. 8.4).

8.4 Clifford–Bézier Formulas

In this section we collect several extensions of the quaternionic approach, showing that they can be unified in the framework of geometric algebra (associated with the most general case of pseudo-Euclidean spaces). Sections 8.4.1–8.4.4 require basic knowledge of geometric algebra (e.g. [7,8,16]). Preliminaries for Sect. 8.4.5 include elements of Laguerre geometry and Pythagorean-normal surfaces [12, 17, 18].

8.4.1 Pseudo-Euclidean Space and Its Geometric Algebra

A *pseudo-Euclidean* space is a vector space $\mathbb{R}^n_\sigma$, with a scalar (interior) product having signature $\sigma = (n_+, n_-, n_0)$, $n = n_+ + n_- + n_0$, i.e. with an orthonormal basis $\{e_1, \ldots, e_n\}$, such that

$$e_i \cdot e_i = \begin{cases} 1, & \text{if } i \le n_+, \\ -1, & \text{if } n_+ + 1 \le i \le n_+ + n_-, \\ 0, & \text{if } i > n_+ + n_-, \end{cases} \quad e_i \cdot e_j = 0,\ i \ne j. \tag{8.19}$$

An abbreviated notation for signature will be used $\sigma = (n) = (n, 0, 0)$ and $\sigma = (n_+, n_-) = (n_+, n_-, 0)$.

Define a *geometric algebra* $\mathcal{G}_\sigma = \mathcal{G}(\mathbb{R}^n_\sigma)$ as a Clifford algebra generated by the pseudo-Euclidean space $\mathbb{R}^n_\sigma$ with a signature $\sigma = (n_+, n_-, n_0)$. The *geometric* product is defined to be associative and distributive with respect to addition, with the extra relation for vectors $v \cdot v = v^2 \in \mathbb{R}$. If $v, u \in \mathbb{R}^n_\sigma$ then the geometric product is a sum of interior and exterior (see below) products

$$vu = v \cdot u + v \wedge u. \tag{8.20}$$

The algebra $\mathcal{G}_\sigma$ has the same underlying vector space as the usual exterior algebra $\bigwedge(\mathbb{R}^n_\sigma)$, namely it is a vector space of dimension 2^n, that can be decomposed as a direct sum $E_0 \oplus E_1 \oplus \cdots \oplus E_n$ of subspaces with the following bases

$$\{1\}, \quad \{e_1, \ldots, e_n\}, \quad \{e_{ij} \mid i < j\}, \quad \{e_{ijk} \mid i < j < k\}, \ldots \quad \{I = e_{12\ldots n}\}, \tag{8.21}$$

where $e_{ij\ldots k} = e_i e_j \cdots e_k$. The vector spaces $E_0, \ldots, E_n$ are scalars, vectors, bivectors, etc. respectively. The basis of E_n has only one element $I = e_1 e_2 \cdots e_n$, which is called a *pseudoscalar*. A *dual* of $x \in \mathcal{G}_\sigma$ is $x^* = Ix$. For any $x \in \mathcal{G}_\sigma$, its k-grade component $\langle x \rangle_k$ is the projection to the subspace E_k of grade k.

A *reversion* operation in the algebra $\mathcal{G}_\sigma$ is defined as follows (see [7, 8, 16] for details). If x is a product of vectors $x = v_1 v_2 \cdots v_{n-1} v_n$, then its reversion is $\tilde{x} = v_n v_{n-1} \cdots v_2 v_1$. If all v_i are non-zero, then $x\tilde{x} = (v_n \cdot v_n) \cdots (v_2 \cdot v_2)(v_1 \cdot v_1) \in \mathbb{R}$. Hence it is easy to calculate the inverse element $x^{-1} = \tilde{x}/(x\tilde{x})$.

8.4.2 Möbius Transformations in $\mathbb{R}^n_\sigma$

A group of *Möbius transformations* Möb$(\mathbb{R}^n_\sigma)$ of a pseudo-Euclidean space $\mathbb{R}^n_\sigma$ is generated by: pseudo-Euclidean reflections, translations, dilatations, and special inversions

$$R_v(x) = -vxv, \quad T_a(x) = x + a, \quad S_r(x) = rx, \quad \mathrm{inv}(x) = x^{-1}, \tag{8.22}$$

where $v, a \in \mathbb{R}^n_\sigma$, $|v| = 1$, $r \in \mathbb{R}_+$. Note the different sign in the inversion formula compared with the quaternionic case (8.1).

Similar to Sect. 8.2.2 M-transformations of $\mathbb{R}^n_\sigma$ can be represented by 2×2 matrices A (with entries in $\mathcal{G}_\sigma$) and corresponding fractional-linear functions Φ_A, see (8.2).

We define *Clifford–Bézier surfaces* (CB-surfaces) by the same rational Bézier formulas treating them as formulas in $\mathcal{G}_\sigma$, i.e. with control points $p_{ij} \in \mathbb{R}^n_\sigma$ and weights $w_{ij} \in \mathcal{G}_\sigma$.

Proposition 8.6 *CB formulas* $(\sum_i p_i w_i B_i)(\sum_i w_i B_i)^{-1}$ *with control points* $p_i \in \mathbb{R}^n_\sigma$ *and weights* $w_i \in \mathcal{G}_\sigma$ *(with certain kind of Bernstein polynomials* B_i*) are mapped by an M-transformation* $\Phi(x) = (ax+b)(cx+d)^{-1}$ *to the same formulas with new control points* $p'_i = \Phi(p_i)$ *and new weights* $w'_i = \hat{\Phi}(p_i, w_i) = (cp_i + d)w_i$.

8.4.3 $\mathbb{C}$ and $\mathbb{H}$ as Subalgebras of Geometric Algebras

Complex numbers $\mathbb{C}$ are identified with an even subalgebra of $\mathcal{G}_2$:

$$\mathrm{in}_{\mathbb{C}} : \mathbb{C} \to (\mathcal{G}_2)_{\mathrm{even}}, \quad z = x + y\,\mathrm{i} \mapsto x + ye_{12}. \tag{8.23}$$

Multiplying by e_1 from the right, one can get the standard map from $\mathbb{C}$ to $\mathbb{R}^2$:

$$\mathrm{in}_{\mathbb{C}} : \mathbb{C} \to \mathbb{R}^2, \quad z = x + y\,\mathrm{i} \mapsto e_1 \mathrm{in}_{\mathbb{C}}(z) = xe_1 + ye_2.$$

Hence any complex Bézier formula can be mapped to a Clifford–Bézier one

$$e_1 \mathrm{in}_{\mathbb{C}}\big((\textstyle\sum_i p_i w_i B_i)(\sum_i w_i B_i)^{-1}\big) = (\sum_i p'_i w'_i B_i)(\sum_i w'_i B_i)^{-1}, \tag{8.24}$$

where $p'_i = e_1 \mathrm{in}_{\mathbb{C}}(p_i)$, and $w'_i = \mathrm{in}_{\mathbb{C}}(w_i)$.

Quaternions $\mathbb{H}$ are identified with an even subalgebra of $\mathcal{G}_3$:

$$\mathrm{in}_{\mathbb{H}} : \mathbb{H} \to (\mathcal{G}_3)_{\mathrm{even}}, \quad q = r + x\,\mathrm{i} + y\,\mathrm{j} + z\,\mathrm{k} \mapsto r - xe_{23} + ye_{13} - ze_{12}. \tag{8.25}$$

Using duality $X^* = IX$, one can get the standard map from imaginary quaternions $\mathrm{Im}\,\mathbb{H}$ to $\mathbb{R}^3$:

$$x\,\mathrm{i} + y\,\mathrm{j} + z\,\mathrm{k} \mapsto I\,\mathrm{in}_{\mathbb{H}}(q) = xe_1 + ye_2 + ze_3.$$

Hence any Quaternionic-Bézier formula can be mapped to a Clifford–Bézier one

$$I\,\mathrm{in}_{\mathbb{H}}\big((\textstyle\sum_i p_i w_i B_i)(\sum_i w_i B_i)^{-1}\big) = (\sum_i p'_i w'_i B_i)(\sum_i w'_i B_i)^{-1}, \tag{8.26}$$

where $p'_i = I\,\mathrm{in}_{\mathbb{H}}(p_i)$, and $w'_i = \mathrm{in}_{\mathbb{H}}(w_i)$.

Therefore all the results from Sects. 8.2 and 8.3 about QB curves and surfaces are valid for the corresponding CB curves and surfaces in the algebra $\mathcal{G}_3$ generated by the Euclidean space $\mathbb{R}^3$ with signature $(3, 0, 0)$.

There are just a couple differences in the formulas:

- Conjugation $q \mapsto \bar{q}$ in $\mathbb{H}$ should be changed to reversion $x \mapsto \tilde{x}$ in $\mathcal{G}_3$,
- The inversion $q \mapsto -q^{-1}$ in $\mathrm{Im}\,\mathbb{H}$ should be changed to $x \mapsto x^{-1}$ in $\mathbb{R}^3 \subset \mathcal{G}_3$.

8.4.4 Conformal Model of Euclidean Space

We are going to demonstrate how our methods can be applied to representing the usual rational Bézier curves and surfaces in the conformal model.

Consider a pseudo-Euclidean space $\mathbb{R}^5_{4,1}$ and its generated geometric algebra $\mathcal{G}_{4,1}$. The standard basis $\{e_1,\dots,e_5\}$, $e_i\cdot e_i=1$, $i\neq 5$, $e_5\cdot e_5=-1$, will be changed to the following one

$$\{e_0,e_1,e_2,e_3,e_\infty\},\quad e_0=(-e_4+e_5)/2,\quad e_\infty=e_4+e_5.$$

Define an embedding of Euclidean space $\mathbb{R}^3$ to $\mathbb{R}^5_{4,1}$:

$$\mathrm{conf}(x)=x+\tfrac{1}{2}x^2e_\infty+e_0 \tag{8.27}$$

to a quadric of null-vectors

$$X\cdot X=0,\quad X\in\mathbb{R}^5_{4,1}. \tag{8.28}$$

If we expand X in the standard basis $X=\sum_i x_ie_i$ then $X\cdot X=x_1^2+\cdots+x_4^2-x_5^2$. Hence the quadric (8.28) defines a 3-sphere S^3 in the affine part $x_5\neq 0$ of the associated projective space $\mathbb{R}P^4=P(\mathbb{R}^5_{4,1})$. Actually $\mathrm{conf}:\mathbb{R}^3\to S^3$ is the inverse of stereographic projection.

Let us apply the machinery we developed. Using the identities $xe_\infty+e_\infty x=0$ and $e_\infty^2=0$, one can modify formula (8.27) as the composition of two fractional-linear functions

$$\mathrm{conf}(x)=x(\tfrac{1}{2}xe_\infty+1)+e_0=x(\tfrac{1}{2}e_\infty x+1)^{-1}+e_0.$$

Hence, the map $\mathrm{conf}:\mathbb{R}^3\to\mathbb{R}^5_{4,1}$ is the restriction of a Möbius transformation $\Phi_C\in\mathrm{Möb}(\mathbb{R}^5_{4,1})$ given by the matrix:

$$C=\begin{pmatrix}1+\frac{1}{2}e_0e_\infty & e_0\\ \frac{1}{2}e_\infty & 1\end{pmatrix}=\begin{pmatrix}1 & e_0\\ 0 & 1\end{pmatrix}\begin{pmatrix}1 & 0\\ \frac{1}{2}e_\infty & 1\end{pmatrix}.$$

Therefore, according to Proposition 8.6 one can 'lift' any CB-curve or surface (including the usual rational Bézier curves and surfaces with real weights) to the conformal model. Indeed new control points P_i and weights W_i are related to the old ones p_i and w_i as follows:

$$P_i=\mathrm{conf}(p_i),\quad W_i=(\tfrac{1}{2}p_ie_\infty+1)w_i. \tag{8.29}$$

The main advantage of this conformal model (i.e. $\mathbb{R}^3$ embedded into $\mathbb{R}^5_{4,1}$) is in the possibility to represent important geometric objects and transformations in $\mathbb{R}^3$ as formulas in the algebra $\mathcal{G}_{4,1}$ (see e.g. [7,8,16]). For example, the conformal image of a circle $C \subset \mathbb{R}^3$ going through three points p_i, $i = 0, 2, 3$, is the intersection of S^3: $X \cdot X = 0$ with a 2-plane $\Pi \wedge X = 0$, where $\Pi = \mathrm{conf}(p_0) \wedge \mathrm{conf}(p_1) \wedge \mathrm{conf}(p_2)$ is a 3-vector. We treat the 3-vector $\Pi \in \mathcal{G}_3$ as a 2-plane and say that it is *associated* with the circle C.

Let us demonstrate how this technique can help us to find a quadratic cone containing the conformal image $\mathrm{conf}(P(s,t))$ of a bilinear CB-patch (cf. Sect. 8.3.3). Using formulas (8.29) we lift the control points p_i and weights w_i given by (8.15) to the corresponding control points P_i and weights W_i in the conformal model. We also compute tangent vectors $V_{ij} = (P_j - P_i)W_j W_i^{-1}$ (see (8.9)). Then the 3-vectors $\Pi_{01} = P_0 \wedge P_1 \wedge V_{01}$, $\Pi_{23} = P_2 \wedge P_3 \wedge V_{23}$ represent 2-planes associated with the opposite boundary circles C_{01} and C_{23} from the same family (in the notation of Lemma 8.3). The family of 2-planes associated with the paired family of circles can be obtained using the classical Steiner construction by intersecting two pencils of hyperplanes defined by the 2-planes Π_{01} and Π_{23}. We have two obvious corresponding pairs of hyperplanes in these pencils: $\Pi_{01} \wedge V_{02}, \Pi_0 \wedge P_2$ and $\Pi_{23} \wedge P_0, \Pi_2 \wedge V_{20}$. Hence the implicit equation of the quadric cone we are looking for should be the determinant of these four hyperplanes:

$$(\Pi_{01} \wedge V_{02} \wedge X)(\Pi_{23} \wedge V_{20} \wedge X) - (\Pi_{01} \wedge P_2 \wedge X)(\Pi_{23} \wedge P_0 \wedge X) = 0.$$

Of course in order to fix a correct projective correspondence between the pencils one needs three corresponding hyperplanes on these pencils. So in general a certain additional coefficient will be needed in the above equation. In our case the coefficient is 1 by the magic of geometric algebra.

8.4.5 CB-Surfaces in Isotropic Space and PN-Surfaces

In this Section we survey results of [15] on CB-surfaces based on the geometric algebra $\mathcal{G}_{2,0,1}$ generated by an *isotropic space* $\mathbb{R}^3_{2,0,1}$.

The signature $\sigma = (2, 0, 1)$ means that $x \cdot x = x_1^2 + x_2^2$ in coordinates of the standard basis (see (8.19)). Therefore, distances in *isotropic geometry* are measured as Euclidean distances in the projection to the first two coordinates, which is called a *top view*. *Isotropic Möbius* (i-M) transformations are elements of the group $\mathrm{Möb}(\mathbb{R}^3_{(2,0,1)})$ as defined in Sect. 8.4.2. The distinguished vertical direction separates all planes into two classes: vertical (isotropic) and non-vertical planes. Images of these two classes of planes under i-M transformations generate two types of *isotropic spheres* (i-spheres): paraboloids of revolution with a vertical axis (parabolic type) and cylinders with top view circles (cylindrical type). An *isotropic*

circle (i-circle) is the intersection between an i-sphere of parabolic type and a plane: it is either an ellipse with a circle as top view or a parabola with a vertical axis.

It appears that the theory of QB-surfaces developed in Sects. 8.2 and 8.3 (and initially introduced in [13]) can be successfully developed in the case of CB-surfaces in isotropic space. In general one just needs to add everywhere 'isotropic', e.g. circles and M-transformations should be changed to i-circles and i-M-transformations. The counterpart of a Dupin cyclide is an *isotropic cyclide*: a quartic surface in $\mathbb{R}^3_{2,0,1}$ with a double conic $x_1^2 + x_2^2 = 0$ at infinity or its i-M-transformations.

In [15] bilinear CB-patches in $\mathbb{R}^3_{2,0,1}$ are studied in much detail: their implicitization formula is derived, they are characterized as patches on isotropic cyclides and the uniqueness of patches with three given boundary isotropic circles is proved.

The motivation for these studies is in the following theorem due to Pottmann and Peternell [17, 18]:

Theorem 8.5 *The duality* (8.30) *defines a 1–1 correspondence between non-developable PN-surfaces in the Euclidean space* $\mathbb{R}^3$ *and rational surfaces in the isotropic space* $\mathbb{R}^3_{2,0,1}$.

We recall here PN-surfaces and the construction of duality. *Pythagorean-normal* (PN) surfaces are rational surfaces in the Euclidean space $\mathbb{R}^3$ together with a field of rational unit normals. PN-surfaces are important in geometric modeling applications, since they are rational surfaces with rational offsets. Following [17, 18] (see also survey in [12]), we map oriented planes in $\mathbb{R}^3$ to points of the isotropic space

$$n_1x_1 + n_2x_2 + n_3x_3 + h = 0 \mapsto \frac{1}{n_3 + 1}(n_1, n_2, h) \in \mathbb{R}^3_{2,0,1}. \tag{8.30}$$

Treating a surface in $\mathbb{R}^3$ as the set of its oriented tangent planes, then applying the map (8.30) we get a *dual* surface in $\mathbb{R}^3_{2,0,1}$

We end this exposition with one PN-surface modeling example.

Example 8.2 Consider a corner defined by three orthogonal planes, where three edges are blended using cylinders of radii $r_1 < r_2 < r_3$. The goal is to find a quadrangular PN-patch that will blend smoothly the given three cylinders and the top horizontal plane as shown in Fig. 8.5. The idea is to apply duality (8.30): the cylinders go to i-circular arcs and the top plane goes to a point in the isotropic space. Using the isotropic analog of Lemma 8.3 (see [15, Theorem 1]), one can fill the triangular contour shown in Fig. 8.5 (left) with a bilinear CB-patch and go back using duality. The resulting PN-surface patch can be represented as a Bézier surface of bidegree (3, 4), Fig. 8.5 (right).

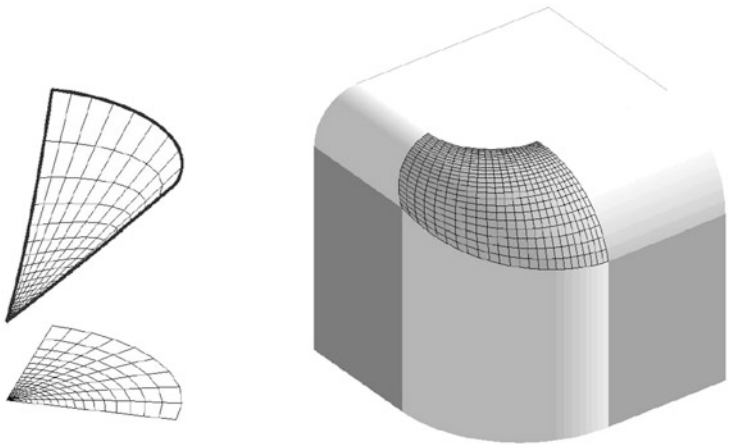

Fig. 8.5 A CB-patch (with a top view) and its dual PN-surface patch

Conclusions
We introduced quaternionic Bézier curves and surfaces in Euclidean space $\mathbb{R}^3$ with two main advantages compared to the customary rational Bézier case: more compact representation (the degree is halved) and Möbius invariance. Disadvantages include absence of affine invariance and complicated conditions on control points and weights that keep quaternionic Bézier curves and surfaces in $\mathbb{R}^3$.

The simplest non-trivial case of bilinear quaternionic Bézier patches was studied:

- The implicitization formula is presented;
- They are characterized as Darboux cyclide patches;
- All such patches on a given Darboux cyclide are classified;
- Principal patches on Dupin cyclides are presented in this form.

We also have shown that complex or quaternionic Bézier formulas can be translated to more general geometric algebra settings. This approach is useful for representing usual rational Bézier curves and surfaces in the conformal model, and for understanding bilinear Clifford–Bézier patches in isotropic space, which have potential applications to rational offset surface modeling.

Acknowledgements The authors would like to thank Helmut Pottmann for pointing out that general bilinear quaternionic patches may represent Darboux cyclides and providing access to the preliminary version of [19]. The majority of the numerical experiments and symbolic computations were made for this paper using the software package CLUCalc/CLUViz described in [16] and the MAPLE package Clifford [1].

References

1. R. Ablamowicz, B. Fauser, A Maple 10 Package for Clifford Algebra Computations, Version 10 (2007). http://math.tntech.edu/rafal/cliff10
2. G. Albrecht, W.L.F. Degen, Construction of Bézier rectangles and triangles on the symmetric Dupin horn cyclide by means of inversion. Comput. Aided Geom. Des. **14**, 349–375 (1997)
3. C. Bisi, G. Gentili, Moebius transformations and the poincare distance in the quaternionic setting. Indiana Univ. Math. J. **58**, 2729–2764 (2010)
4. A. Bobenko, U. Pinkall, Discrete isothermic surfaces. J. Reine Angew. Math. **475**, 187–208 (1996)
5. W. Degen, Cyclides, in *Handbook of Computer Aided Geometric Design* (Elsevier, Amsterdam/Boston, 2002), pp. 575–601
6. R. Dietz, J. Hoschek, B. Juettler, An algebraic approach to curves and surfaces on the sphere and on other quadrics. Comput. Aided Geom. Des. **10**, 211–229 (1993)
7. L. Dorst, D. Fontijne, S. Mann, *Geometric Algebra for Computer Science* (Morgan-Kaufmann, San Francisco, 2007)
8. R. Goldman, A Homogeneous model for three-dimensional computer graphics based on the clifford algebra for $\mathbb{R}^3$, in *Guide to Geometric Algebra in Practice*, ed. by L. Dorst, J. Lasenby (Springer, New York, 2011), pp. 329–352
9. V. Karpavičius, R. Krasauskas, Real-time visualization of Möbius transformations in space using Quaternionic-Bézier approach, in *21-st International Conference on Computer Graphics, Visualization and Computer Vision (WSCG), Communication Papers Proceedings*, Pilsen, 2013, pp. 259–266. http://wscg.zcu.cz/wscg2013/program/short/C17-full.pdf
10. R. Krasauskas, Bézier patches on almost toric surfaces, in *Algebraic Geometry and Geometric Modeling* (Springer, Berlin/New York, 2006), pp. 135–150
11. R. Krasauskas, C. Maeurer, Studying cyclides with laguerre geometry. Comput. Aided Geom. Des. **17**, 101–126 (2000)
12. R. Krasauskas, M. Peternell, Rational offset surfaces and their modeling applications, in *IMA Volume 151: Nonlinear Computational Geometry*, ed. by I.Z. Emiris, F. Sottile, T. Theobald (Springer, New York, 2010), pp. 109–135
13. R. Krasauskas, S. Zube, Bézier-like parametrizations of spheres and cyclides using geometric algebra, in *Proceedings of 9th International Conference on Clifford Algebras and Their Applications in Mathematical Physics*, Weimar, 2011, ed. by K. Guerlebeck
14. R. Krasauskas, S. Zube, Representation of Dupin cyclides using quaternions (in preparation)
15. R. Krasauskas, S. Zube, S. Cacciola, Bilinear Clifford-Bézier patches on isotropic cyclides, in *Mathematical Methods for Curves and Surfaces*. LNCS, vol. 8177, ed. by M. Floater et al. (Springer, Berlin/Heidelberg, 2014), pp. 283–303
16. C. Perwass, *Geometric Algebra with Applications in Engineering*. Series: geometry and computing, vol. 4 (Springer, Berlin/Heidelberg, 2009)
17. M. Peternell, H. Pottmann, A Laguerre geometric approach to rational offsets. Comput. Aided Geom. Des. **15**, 223–249 (1998)
18. H. Pottmann, M. Peternell, Applications of Laguerre geometry in CAGD. Comput. Aided Geom. Des. **15**, 165–186 (1998)
19. H. Pottmann, L. Shi, M. Skopenkov, Darboux cyclides and webs from circles. Comput. Aided Geom. Des. **29**, 77–97 (2012)
20. J. Sanchez-Reyes, Complex rational Bézier curves. Comput. Aided Geom. Des. **26**, 865–876 (2009)
21. S. Zube, A circle representation using complex and quaternion numbers. Lith. J. Math. **46**, 298–310 (2006)
22. S. Zube, Quaternionic rational Bézier curves. Lietuvos matematikos rinkinys **52**, 53–58 (2011)